White Rose Research Online

eprints@whiterose.ac.uk
https://eprints.whiterose.ac.uk
Universities of Leeds, Sheffield and York

Deposited via The University of Sheffield.

White Rose Research Online URL for this paper:
https://eprints.whiterose.ac.uk/id/eprint/203651/

Version: Published Version

Article:
Moher Alsady, T., Voskrebenzev, A., Behrendt, L. et al. (2024) Multicenter standardization of phase-resolved functional lung MRI in patients with suspected chronic thromboembolic pulmonary hypertension. Journal of Magnetic Resonance Imaging, 59 (6). pp. 1953-1964. ISSN: 1053-1807

https://doi.org/10.1002/jmri.28995

Reuse
This article is distributed under the terms of the Creative Commons Attribution (CC BY) licence. This licence allows you to distribute, remix, tweak, and build upon the work, even commercially, as long as you credit the authors for the original work. More information and the full terms of the licence here: https://creativecommons.org/licenses/

Takedown
If you consider content in White Rose Research Online to be in breach of UK law, please notify us by emailing eprints@whiterose.ac.uk including the URL of the record and the reason for the withdrawal request.

UNIVERSITY OF LEEDS
University of Sheffield
UNIVERSITY of York

Check for updates

RESEARCH ARTICLE

Multicenter Standardization of Phase-Resolved Functional Lung MRI in Patients With Suspected Chronic Thromboembolic Pulmonary Hypertension

Tawfik Moher Alsady, MD,[1,2] Andreas Voskrebenzev, PhD,[1,2] Lea Behrendt, MS,[1,2] Karen Olsson, MD,[2,3] Claus Peter Heußel, MD,[4] Ekkehard Gruenig, MD,[4] Henning Gall, MD,[5] Ardeschir Ghofrani, MD,[5] Fritz Roller, MD,[6] Sebastian Harth, MD,[6] Helen Marshall, PhD,[7] Paul J.C. Hughes, PhD,[7] Jim Wild, PhD,[7] Andrew J. Swift, MD PhD,[7] David G. Kiely, MD,[8] Jürgen Behr, MD,[9] Julien Dinkel, MD,[10] Dietrich Beitzke, MD,[11] Irene M. Lang, MD,[12] Kai Helge Schmidt, MD,[13] Karl Friedrich Kreitner, MD,[14] Thomas Frauenfelder, MD,[15] Silvia Ulrich, MD,[16] Okka W. Hamer, MD,[17] and Jens Vogel-Claussen, MD[1,2]*

Background: Detection of pulmonary perfusion defects is the recommended approach for diagnosing chronic thromboembolic pulmonary hypertension (CTEPH). This is currently achieved in a clinical setting using scintigraphy. Phase-resolved functional lung (PREFUL) magnetic resonance imaging (MRI) is an alternative technique for evaluating regional ventilation and perfusion without the use of ionizing radiation or contrast media.
Purpose: To assess the feasibility and image quality of PREFUL-MRI in a multicenter setting in suspected CTEPH.
Study Type: This is a prospective cohort sub-study.
Population: Forty-five patients (64 ± 16 years old) with suspected CTEPH from nine study centers.
Field Strength/Sequence: 1.5 T and 3 T/2D spoiled gradient echo/bSSFP/T2 HASTE/3D MR angiography (TWIST).
Assessment: Lung signal-to-noise ratio (SNR) and contrast-to-noise ratio (CNR) were compared between study centers with different MRI machines. The contrast between normally and poorly perfused lung areas was examined on PREFUL images. The perfusion defect percentage calculated using PREFUL-MRI (QDP_{PREFUL}) was compared to QDP from the established dynamic contrast-enhanced MRI technique (QDP_{DCE}). Furthermore, QDP_{PREFUL} was compared between a patient subgroup with confirmed CTEPH or chronic thromboembolic disease (CTED) to other clinical subgroups.
Statistical Tests: *t*-Test, one-way analysis of variance (ANOVA), Pearson's correlation. Significance level was 5%.
Results: Significant differences in lung SNR and CNR were present between study centers. However, PREFUL perfusion images showed a significant contrast between normally and poorly perfused lung areas (mean delta of normalized perfusion −4.2% SD 3.3) with no differences between study sites (ANOVA: $P = 0.065$). QDP_{PREFUL} was significantly correlated

View this article online at wileyonlinelibrary.com. DOI: 10.1002/jmri.28995

Received Jun 12, 2023, Accepted for publication Aug 21, 2023.

*Address reprint requests to: J.V.C., Institute for Radiology, Carl-Neuberg-Strasse 1, 30625 Hannover, Germany. E-mail: vogel-claussen.jens@mh-hannover.de

From the [1]Institute for Diagnostic and Interventional Radiology, Hannover Medical School, Hannover, Germany; [2]Biomedical Research in End-Stage and Obstructive Lung Disease (BREATH), German Center for Lung Research, Hannover, Germany; [3]Department of Respiratory Medicine, Hannover Medical School, Hannover, Germany; [4]Thoraxklinik, University Hospital of Heidelberg, Heidelberg, Germany; [5]Department of Internal Medicine, University Hospital Giessen, Giessen, Germany; [6]Department of Diagnostic and Interventional Radiology, University Hospital Giessen, Giessen, Germany; [7]Department of Infection, Immunity and Cardiovascular Disease, University of Sheffield, Sheffield, UK; [8]Sheffield Pulmonary Vascular Disease Unit, NIHR Biomedical Research Centre Sheffield, Sheffield, UK; [9]Department of Medicine V, University Hospital of Munich, Munich, Germany; [10]Department of Radiology, University Hospital of Munich, Munich, Germany; [11]Department of Biomedical Engineering and Image-Guided Therapy, Medical University of Vienna, Vienna, Austria; [12]Internal Medicine II, AKH-Vienna, Medical University of Vienna, Vienna, Austria; [13]Cardiology I, University Medical Centre, Johannes Gutenberg University Mainz, Mainz, Germany; [14]Department of Diagnostic and Interventional Radiology, University Medical Centre, Johannes Gutenberg University Mainz, Mainz, Germany; [15]Institute for Diagnostic and Interventional Radiology, University Hospital Zurich, Zurich, Switzerland; [16]Department of Pulmonology, University Hospital Zurich, Zurich, Switzerland; and [17]Institute for Radiology, University Hospital Regensburg, Regensburg, Germany

This is an open access article under the terms of the Creative Commons Attribution License, which permits use, distribution and reproduction in any medium, provided the original work is properly cited.

© 2023 The Authors. *Journal of Magnetic Resonance Imaging* published by Wiley Periodicals LLC on behalf of International Society for Magnetic Resonance in Medicine.

with QDP_{DCE} ($r = 0.66$), and was significantly higher in 18 patients with confirmed CTEPH or CTED (57.9 ± 12.2%) compared to subgroups with other causes of PH or with excluded PH (in total 27 patients with mean ± SD QDP_{PREFUL} = 33.9 ± 17.2%).
Data Conclusion: PREFUL-MRI could be considered as a non-invasive method for imaging regional lung perfusion in multi-center studies.
Level of Evidence: 3
Technical Efficacy: Stage 1

J. MAGN. RESON. IMAGING 2023.

Phase-resolved functional lung (PREFUL) magnetic resonance imaging (MRI) is a non-invasive imaging technique for evaluating regional dynamics of pulmonary ventilation and perfusion.[1] PREFUL-MRI is usually acquired using a spoiled gradient echo sequence in free tidal breathing without the need for contrast media. This technique has been successfully implemented in a fully automatic post-processing framework for estimation of normalized regional pulmonary perfusion.[2] PREFUL-MRI has been previously used to assess postoperative lung perfusion improvement in patients with chronic thromboembolic pulmonary hypertension (CTEPH) undergoing pulmonary endarterectomy (PEA).[3] A dual-center study showed the feasibility of using PREFUL-MRI to evaluate lung perfusion in patients with cystic fibrosis and a good agreement with the well-established dynamic contrast-enhanced MRI technique (DCE-MRI) was found.[4] In addition, PREFUL-MRI allows the assessment of regional ventilation dynamics. For example, flow volume loops derived from ventilation-weighted PREFUL-MRI have been previously used to detect regional ventilation defects at early stages of chronic lung allograft dysfunction in lung transplantation patients.[5]

CTEPH is a life-threatening long-term complication of acute pulmonary embolism (PE).[6,7] The clinical outcomes can however be greatly improved if the disease is treated early enough mainly with a surgical approach named pulmonary endarterectomy (PEA)[8,9] or alternative interventions such as balloon pulmonary angioplasty and/or medical treatment in cases where surgery is not feasible.[10] Diagnosing CTEPH requires, among others, the detection of non-matched segmental and subsegmental perfusion deficits within the pulmonary arterial tree (ventilation-perfusion mismatch) due to chronic PEs. This is currently achieved in a clinical setting using ventilation-perfusion single-photon emission computed tomography (VQ-SPECT) which is still considered the reference standard.[11,12] Besides a usually lower availability than other imaging techniques like CT pulmonary angiography (CTPA), the main disadvantage of VQ-SPECT is radiation exposure. An alternative that does not require ionizing radiation is the 3D DCE-MRI, which has been proven by single-center studies to have a high sensitivity equivalent to perfusion scintigraphy in diagnosing CTEPH.[13,14] A European multi-centric study named CHANGE-MRI ClinicalTrials.gov identifier NCT02791282) aims to assess the diagnostic value of MRI in comparison to VQ-SPECT in suspected CTEPH.[15] Within the scope of this study, PREFUL and DCE-MRI datasets were acquired to facilitate the validation of PREFUL in a multi-center context using DCE-MRI and VQ-SPECT as a reference.

Therefore, the aim of this substudy is to assess the feasibility and image quality of PREFUL-MRI datasets acquired in a multi-center setting for screening patients with suspected CTEPH.

Materials and Methods

Study Population

The study was approved by the Institutional Review Boards at all participating centers and a written informed consent was obtained from all participants. The CHANGE-MRI cohort included adult patients (>18 years old) with clinical suspicion for CTEPH. Exclusion criteria were known contraindications for contrast-enhanced MRI, such as those with cardiac pacemakers, claustrophobia, hypersensitivity to intravenous MR contrast agents, and pregnant or breastfeeding women. All study participants underwent MRI and VQ-SPECT imaging. In participants with positive MRI or VQ-SPECT findings, the presence of PEs was verified by CTPA and/or conventional pulmonary angiography (CPA). A reference standard for the final diagnosis was defined in the CHANGE-MRI study as a diagnostic strategy with VQ-SPECT as a screening test and CPA/CTPA as a verification test, corrected by clinical diagnosis after 6–12 months.[15]

For this study, a total of 45 patients were randomly chosen from the nine European CHANGE-MRI study sites (5 patients from each site, in total 24 females and 21 males, mean age 64 ± 16, age range 28–84 years). According to the reference standard of the CHANGE-MRI study, 17 patients were diagnosed with CTEPH and 1 patient with chronic thromboembolic pulmonary vascular disease (CTED). Patients with CTED exhibit, as those with CTEPH, non-matched segmental and subsegmental perfusion deficits, however, without a manifesting pulmonary hypertension component. The study cohort included 11 patients who were eventually diagnosed with pulmonary arterial hypertension (PAH). In eight patients, other causes of pulmonary hypertension (PH) were found. Regardless of the presence of PH, five patients in the study cohort had diagnosed COPD. Clinical data including the endpoint diagnosis of the selected patients are summarized in Tables 1 and 2.

MRI Acquisition

MRI scanners at study sites were either 1.5 T or 3 T from different vendors (see Table 3). Each patient underwent an MRI scan of the thorax. The MRI protocol was the same across study sites and included: anatomical sequences in both axial and coronal planes

15222586, 0, Downloaded from https://onlinelibrary.wiley.com/doi/10.1002/jmri.28995 by Test, Wiley Online Library on [27/09/2023]. See the Terms and Conditions (https://onlinelibrary.wiley.com/terms-and-conditions) on Wiley Online Library for rules of use; OA articles are governed by the applicable Creative Commons License

TABLE 1. Participant Characteristics in the Sub-Study Cohort

(Site ID) Study Center	Mean Age ± SD (Years)	PH Positive (N)	CTEPH Positive (N)	MRI Protocol Successful (N)
(01) BREATH—Hannover	72 ± 9	4	0	5
(02) TLRC—Heidelberg	70 ± 15	4	3	5
(03) UGMLC—Giessen	47 ± 17	3	1	5
(04) USFD—Sheffield	68 ± 13	4	3	5
(05) CPC—Munich	55 ± 19	4	2	5
(06) AKH—Vienna	64 ± 18	5	2	5
(07) JGU—Mainz	73 ± 12	5	1	5
(08) USZ—Zurich	59 ± 12	2	2 (+1 CTED)	5
(09) UKR—Regensburg	66 ± 17	5	3	5

PH and CTEPH diagnosis were established based on reference standard imaging (pulmonary angiography/CTPA), or when not available, in accordance with the VQ-SPECT results. From each center, five participants were included.
PH = pulmonary hypertension; CTED = chronic thromboembolic pulmonary disease; CTEPH = chronic thromboembolic pulmonary hypertension.

using balanced steady-state free precession (bSSFP) and T2-weighted half Fourier single-shot turbo spin-echo (HASTE) sequences, functional lung imaging using PREFUL technique with a coronal 2D spoiled gradient-echo (GRE) sequence (known as fast low angle shot; FLASH), cardiac imaging involved cine bSSFP in four chamber view and short axis orientation, 3D DCE-MRI using time-resolved angiography with interleaved stochastic trajectories (TWIST) and pulmonary MR angiography (3D GRE). Array coils with 8–12 channels were used for the study. For a detailed description of the MRI protocol and the used parameters for all acquired sequences, see the study design publication.[15] The sequence parameters for PREFUL imaging are also described in the following paragraph.

PREFUL acquisitions included multiple 2D coronal slices covering whole lungs as well as a mid-sagittal slice of each lung. Table 3 includes a summary of the scan parameters of the spoiled GRE sequence for PREFUL, which were: repetition time 3 msec, echo time <0.9 msec, flip angle 5°, slice thickness 15 mm, slice gap 33%, field-of-view 500 × 500 mm, matrix 128 × 128, generalized autocalibrating partially parallel acquisitions (GRAPPA) with 2-fold acceleration (except for the Sheffield site without parallel imaging) and totally 250 frames per slice with a temporal resolution of 288 msec. As seen in Table 3, slightly different acquisition parameters were used at some of the study sites.

Post-Processing and PREFUL Analysis

PREFUL datasets from all study sites were processed on a central server (located in Hannover) using a fully automated pipeline. Utilizing a job on a high-performance cluster allocated with 12 CPUs, the entire post-processing and PREFUL analysis pipeline required approximately 20 minutes per slice. The following steps were run independently for each coronal and sagittal slice in the datasets:

1. Group-oriented registration of the acquired time frames[16] using the advanced normalization tools (ANTs) software.[17]
2. Automatic segmentation of lung parenchyma using a previously trained U-NET convolutional neural network.[18]
3. Automatic segmentation of a large vessel region of interest (ROI) for image sorting in a pulse wave and for perfusion normalization[2] using an in-house-developed MATLAB script (R2019b, MathWorks).
4. PREFUL analysis[1] using an in-house-developed MATLAB script (R2019b, MathWorks). PREFUL performed image sorting based on virtual ventilation and perfusion cycles. Then, it calculated a normalized pulse wave throughout the lung parenchyma, regional ventilation time series (RVt) that spanned the whole breathing cycle and regional flow-volume loops (rFVL) consisting of RVt (as a volume surrogate) and RVt slopes (as a flow surrogate). Additionally, 2D movies covering the whole virtual respiration and cardiac cycle were generated (showcasing regional ventilation dynamics and pulse wave).
5. Automated selection of the pulmonary perfusion phase from the virtual pulse wave and calculation of normalized perfusion with arbitrary units (in relation to the large vessel ROI).
6. Estimation of the rFVL-correlation coefficient (rFVL-CC) in all lung voxels in comparison to a healthy reference. The healthy reference was automatically selected as the biggest cluster of voxels with FV values in the of 75th–95th quantile range.
7. Generation of ventilation and perfusion defect maps by applying a threshold to the rFVL-CC images (fixed threshold of 0.9)[5] and to the normalized perfusion map (fixed threshold of 0.2).[4] Ventilation and perfusion defect percentages (VDP_{PREFUL} and QDP_{PREFUL}) were also estimated from the relation between defect areas and whole lung.

In addition, QDP was also calculated from DCE datasets as follows: First, a ROI was manually drawn in the ascending aorta by

15222586, 0, Downloaded from https://onlinelibrary.wiley.com/doi/10.1002/jmri.28995 by Test, Wiley Online Library on [27/09/2023]. See the Terms and Conditions (https://onlinelibrary.wiley.com/terms-and-conditions) on Wiley Online Library for rules of use; OA articles are governed by the applicable Creative Commons License

TABLE 2. Clinical Diagnosis of Study Participant Determined during the 6-Month Follow-Up Visit

PH Positive

Type		N	Cardiopulmonary Comorbidities (N)
Group 1	Idiopathic PAH	11	• O-ILD + bronchial asthma (1) • COPD + CAD (1) • History of PE (1) • CAD (2) • CHF (1)
	Connective tissue disease	1	-
Group 2	Left heart disease	3	• AFib (1) • COPD (1)
	Pulmonary vein stenosis	1	AFib + ASD + history of PE (1)
Group 3	ILD-related	2	History of PE (1)
Group 4	CTEPH	17	• COPD + TAA + history of PE (1) • AFib + history of PE (1) • CAD + AFib + history of PE (1) • CAD + history of PE (1) • Hereditary thrombophilia + CAD + AFib + Bronchial asthma (1) • History of PE (4) • Bronchial asthma (1) • Pulmonary metastasis of RCC (1)
Group 5	Unclear/multifactorial	1	-

PH Negative

Other Pulmonary Diagnosis	N	Cardiovascular Comorbidities (N)
COPD	2	CAD + TAA + AFib (1)
ILD	2	CAD (1)
CTED	1	-
History of PE	3	• Recurrent thrombophlebitis (1) • Elevated factor VIII (1)
None	1	-

Listed types of pulmonary hypertension according to the WHO groups.[11]
PH = pulmonary hypertension; PAH = pulmonary arterial hypertension; PE = pulmonary embolism; COPD = chronic obstructive pulmonary disease; ILD = interstitial lung disease; O-ILD = combined obstructive and interstitial lung disease; CTED = chronic thromboembolic disease; CAD = coronary artery disease; TAA = thoracic aortic aneurysm; AFib = atrial fibrillation; PFO = patent foramen ovale; ASD = atrial septal defect; CHF = chronic heart failure.

a radiologist with 5 years of experience in thoracic imaging (T.M.) using an in-house-developed MATLAB script. Subsequently, the lung perfusion phase was selected based on the signal function observed in the aorta, as previously described in a dual-center study.[4] To compensate the thinner slice thickness of the DCE images compared to the 2D PREFUL images, coronal slice reformations of the perfusion DCE images were generated, corresponding to thickness and location of PREFUL slices. The QDP_{DCE} value was then calculated from these generated coronal DCE slices using the threshold of the 75th quantile multiplied by 0.6.[19]

Image Quality Assessment

A radiologist with 5 years of experience in thoracic imaging (T.M.), a doctoral candidate physicist with 6 years of experience in PREFUL imaging (L.B.) and a senior medical student with 3 years of experience in PREFUL imaging (M.S.) qualitatively examined raw PREFUL datasets. Image quality was assessed with regard to the following aspects:

- *Whole lung coverage*. They determined whether more than one coronal plane of lung parenchyma was acquired (yes) or not (no).

15222586, 0, Downloaded from https://onlinelibrary.wiley.com/doi/10.1002/jmri.28995 by Test, Wiley Online Library on [27/09/2023]. See the Terms and Conditions (https://onlinelibrary.wiley.com/terms-and-conditions) on Wiley Online Library for rules of use; OA articles are governed by the applicable Creative Commons License

TABLE 3. Summary of MRI Scanners Used at Different Study Sites and the Acquisition Parameters for PREFUL-MRI

Site ID—Location	Scanner (Participants)	Field Strength (T)	TR (msec)	TE (msec)	Flip Angle (°)	FOV (mm^2)	Matrix	Slice Thickness (mm)
Study protocol			3	<0.9	5	500 × 500	128 × 128	15
01—Hannover	SIEMENS Aera (N = 3)	1.5	3	0.82	5	500 × 500	128 × 128	15
	SIEMENS Avanto (N = 2)	1.5	3	0.82	5	500 × 500	128 × 128	15
02—Heidelberg	SIEMENS Aera (N = 5)	1.5	3	0.88	5	500 × 500	128 × 128	**10**
03—Giessen	SIEMENS Avanto (N = 5)	1.5	3	**0.92**	5	500 × 500	128 × 128	15
04—Sheffield	GE Signa HDxt (N = 5)	1.5	**2.32**	0.75	**4**	**480 × 480**	**96 × 96**	15
05—Munich	SIEMENS Aera (N = 5)	1.5	3	0.82	5	500 × 500	128 × 128	15
06—Vienna	SIEMENS Avanto fit (N = 5)	1.5	3	0.82	5	500 × 500	128 × 128	15
07—Mainz	SIEMENS Prisma (N = 5)	3	3	0.82	5	500 × 500	128 × 128	15
08—Zurich	SIEMENS Skyra (N = 5)	3	3	0.82	5	500 × 500	128 × 128	15
09—Regensburg	SIEMENS Avanto fit (N = 1)	1.5	3	0.78	5	500 × 500	128 × 128	15
	SIEMENS Avanto (N = 4)	1.5	3	0.78	5	500 × 500	128 × 128	15

Scan parameters on the GE scanner at the Sheffield site were set slightly different from the study protocol in order to obtain a better image quality. Deviations from study protocol are marked in bold.
TR = repetition time; TE = echo time; FOV = field of view.

- *Image artifacts*. They evaluated the presence of artifacts and categorized them as non, mild, or substantial based on the extent to which they obscured the lung parenchyma.
- *Diagnostic image quality*. They determined whether the image quality was sufficient for delineating lung parenchyma and defining main mediastinal structures (yes). If moderate to severe image artifacts overlayed lung parenchyma or in case of inappropriate planning of the slice where parts of the lung were not imaged, they deemed the diagnostic image quality as inadequate (no).

Slice-wise rating of partial volume effects was also performed (0—non-existing/1—mild partial voluming with the chest wall without any substantial obscuring of lung parenchyma and vessels/2—

15222586, 0, Downloaded from https://onlinelibrary.wiley.com/doi/10.1002/jmri.28995 by Test, Wiley Online Library on [27/09/2023]. See the Terms and Conditions (https://onlinelibrary.wiley.com/terms-and-conditions) on Wiley Online Library for rules of use; OA articles are governed by the applicable Creative Commons License

severe obscuring of lung tissue due to partial volume effect). Coronal slices lying outside the lung or having substantial partial volume effects between the lung and thoracic wall were manually excluded from further analysis.

Signal-to-noise ratio (SNR) and contrast-to-noise ratio (CNR) were calculated for expiratory and inspiratory phases of each slice. For each coronal slice, a radiologist (T.M.) delineated ROIs in the background noise adjacent to the thoracic wall, peripheral lung parenchyma, and central (or the most prominent) lung vessels. SNR was calculated as the ratio of mean signal intensity in the lung parenchyma ROI to the mean signal in the background ROI after correcting for the non-central chi distribution in magnitude images of multi-channel receive coils.[20] CNR was calculated as the signal ratio between peripheral lung parenchyma and central lung vessels.

Evaluation of Automated PREFUL Analysis and Results

After completion of automatic PREFUL analyses, three independent observers (mentioned in the previous section) visually rated the processed datasets for correctness of co-registration and lung segmentation. Inaccuracies in the co-registration were rated as mild, moderate, or severe. Similarly, the lung segmentation was evaluated with ratings from relatively accurate to the extent of lung area missed on segmentation (categorized as mild <25%, moderate <50%, or severe >50%) or the presence of non-lung parenchyma areas in the segmentation mask.

Slices with severely non-accurate registration were excluded due to probable miscalculation of the quantified perfusion. Any inaccurate lung segmentation was manually corrected and sent back to the pipeline for reanalysis. The automatically generated large vessel ROIs as well as the automatic selection of the pulmonary perfusion phase were visually inspected at the end of the analysis, In case of inaccuracies, a manual re-segmentation or re-selection was done. Following these manual adjustments, the metrics were recalculated.

In order to assess the contrast between normally and hypoperfused lung parenchyma on PREFUL-MRI perfusion maps, a radiologist (T.M.; 5 years of experience in thoracic imaging) segmented free-shape ROIs on VQ-SPECT images ($ROIs_{(SPECT)}$) using an in-house-developed MATLAB script. These ROIs, representing normally and poorly perfused areas, were replicated on the corresponding PREFUL morphological images. The analysis encompassed a total of 114 coronal slices from 21 patients. Only patients with perfusion defects detected on VQ-SPECT were included in the analysis (N = 21), regardless of a confirmed CTEPH diagnosis (N = 16) or not (N = 5).

Statistical Analysis

Differences in lung SNR and CNR between the study centers were assessed using one-way analysis of variance (ANOVA). As SNR is expected to increase in expiration, differences in lung SNR and CNR between inspiration and expiration were also tested using paired *t*-test.

Differences in normalized perfusion between normally and poorly perfused $ROIs_{(SPECT)}$ were assessed on PREFUL perfusion images using Bland–Altman analysis. In addition, the contrast between normally and poorly perfused $ROIs_{(SPECT)}$ was examined for variations between different study centers using ANOVA test.

QDP_{PREFUL} was compared to QDP_{DCE} using a correlation analysis with Pearson's correlation and a Bland–Altman analysis. In addition, QDP_{PREFUL} was compared using a two-sample *t*-test between patients with confirmed and excluded diagnosis of CTEPH/CTED. QDP_{PREFUL} was also compared between the subgroup with confirmed CTEPH/CTED (expected to have a high perfusion defect percentage) to other patients with excluded CTEPH/CTED and assigned to the following clinical subgroups: confirmed pulmonary arterial hypertension (PAH), other causes of pulmonary hypertension and excluded pulmonary hypertension.

PREFUL parameters of lung ventilation (mean rFVL-CC and VDP) were compared using Pearson's correlation to the following lung function testing scores: forced expiratory volume (FEV1), forced vital capacity (FVC), FEV1/FVC ratio, total lung capacity (TLC), and diffusing capacity for carbon monoxide (DLCO). VDP_{PREFUL} was also compared using two-sample *t*-test between patients with confirmed CTEPH and patients with excluded CTEPH. In addition, VDP_{PREFUL} was compared between patients in the study cohort with known chronic obstructive lung disease (COPD) and two other subgroups with patients without known COPD (either having a confirmed PH of any cause or with excluded PH). was also compared between CTEPH negative and positive patients and between patients in the study cohort with known chronic obstructive lung disease (COPD) and others without COPD using two-sample *t*-test.

In all analyses, a significance level of 5% was set. Whenever applicable, Bonferroni correction for multiple comparisons was used.

Results

MR Image Quality

All of the included 45 participants completed their MRI sessions including PREFUL imaging (representative MRI and perfusion SPECT images are shown in Fig. 1). Image quality of PREFUL acquisitions was visually rated by both readers as diagnostic in all 45 datasets. In two participants (first two participants at site 07) only three coronal PREFUL slices were acquired (a central slice at the tracheal plane, a midventral, and a middorsal plane). In all other participants, full lung coverage was achieved with a range of 7–10 coronal slices. From a total of 386 coronal PREFUL slices from all 45 participants, 68 slices were excluded due to substantial partial volume effect (lung parenchyma with ventral and dorsal ribs). One peripheral slice (specifically, the most posterior coronal lung plane) from a patient at site 03 showed mild ghosting artifacts. However, that particular slice was excluded from the analysis due to partial volume effect caused by the presence of the ribs. In all datasets, no severe artifacts were seen in the raw PREFUL images. Table 4 summarizes the results of the subjective scoring of raw image quality and the automated PREFUL processing.

Statistically significant differences in lung SNR and CNR (in expiration and inspiration) were present between study centers. SNR during both inspiration and expiration was not significantly different between the two sites with 3 T

15222586, 0, Downloaded from https://onlinelibrary.wiley.com/doi/10.1002/jmri.28995 by Test, Wiley Online Library on [27/09/2023]. See the Terms and Conditions (https://onlinelibrary.wiley.com/terms-and-conditions) on Wiley Online Library for rules of use; OA articles are governed by the applicable Creative Commons License

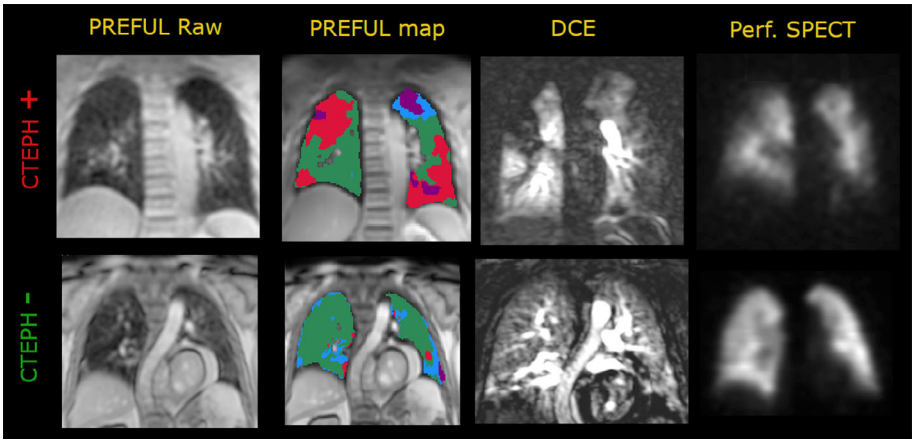

FIGURE 1: Representative MRI and perfusion SPECT slices from a positive and a negative CTEPH patients (scanned at site 04—Sheffield and site 08—Zurich, respectively). Colored PREFUL maps show perfusion defects in red, ventilation defects in blue, and matched defects in violet.

TABLE 4. Subjective Scoring of Raw Images Quality and PREFUL Automated Processing

	Reader 1	Reader 2	Reader 3
Raw MR PREFUL images			
MRI protocol completed (N participants/45)	45 (100%)	-	-
Whole lung scanned (N participants/45)	43 (95.6%)	-	-
Significant partial volume effect (N slices/386)	68 (17.6%)	81 (21%)	52 (13.5%)
Other artifacts (N slices/386)			
Mild	1 (0.3%)	0	2 (0.5%)
Moderate	0	0	0
Severe	0	0	0
Diagnostic image quality (N slices/386)	386 (100%)	386 (100%)	386 (100%)
PREFUL outputs			
Incorrect automatic lung segmentation (N slices/318)			
Mild	2 (0.6%)	-	-
Moderate	0	-	-
Severe	0	-	-
Co-registration inaccuracies (N slices/318)			
Mild	34 (10.7%)	33 (10.3%)	43 (13.5%)
Moderate	1 (0.3%)	0	3 (0.9%)
Severe	0	0	0
Incorrect automatic vessel ROI (N slices/318)	35 (11%)	-	-
Wrong automatic selection of pulmonary perfusion phase (N slices/318)	54 (17%)	-	-

Listed values were the sum of participants or slices that were classified in the corresponding category by the reader. In brackets is the percentage to the total count of participants or slices.
MRI = magnetic resonance imaging; PREFUL = phase-resolved functional lung; ROI = region of interest.

15222586, 0, Downloaded from https://onlinelibrary.wiley.com/doi/10.1002/jmri.28995 by Test, Wiley Online Library on [27/09/2023]. See the Terms and Conditions (https://onlinelibrary.wiley.com/terms-and-conditions) on Wiley Online Library for rules of use; OA articles are governed by the applicable Creative Commons License

scanners (site 07 and 08) and the other seven sites with 1.5 T (two sample *t*-test: $P = 0.204$ in inspiration and $P = 0.106$ in expiration; reported *P*-values before Bonferroni correction for multiple comparisons with N = 4). CNR during both inspiration and expiration was however significantly higher in the datasets from 3 T scanners.

Mean SNR in peripheral lung parenchyma for all 45 participants in expiration was 5.98 (SD 5.88) and in inspiration 3.63 (SD 3.9). Mean CNR between peripheral lung parenchyma and pulmonary vessels in expiration was 17.7 (SD 10.93) and in inspiration 17.52 (SD 11.12). Significantly higher SNR was seen in expiration when compared to inspiration in datasets from all centers (see Fig. 2). In seven out of nine study centers, no statistically significant difference in CNR was found between expiration and inspiration (paired *t*-test $P = 0.285$, 0.128, 0.602, 0.684, 0.432, 0.806, 0.399; *P*-values before applying Bonferroni correction with N = 9; Fig. 2); only in two centers (site 01 and 04), CNR was significantly higher in expiration compared to inspiration.

PREFUL

PREFUL processing of all datasets was successful and normalized maps of lung ventilation and perfusion could be produced. The automatic segmentation of lung parenchyma was mildly (<25% of lung area) inaccurate in only 2/386 slices from different participants scanned at site 01 and 05. These segmentations were manually corrected and the PREFUL analysis was repeated using the corrected segmentation. A total of 33–35 out of 318 slices from different patients showed mild to moderate registration inaccuracies mainly in the form of mild distortion of lung vessels. Upon visual inspection, the automated selection of a vessel ROI for perfusion-weighted analysis was not optimal in 35 out of 318 slices. In most of these cases, the automatic ROI was positioned at the margin of a large vessel, mesenteric fat tissue or in a heart ventricle wall. Similarly, the automated selection of the pulmonary perfusion phase based on the estimated pulse wave was wrong in 54 out of 318 slices. In the latter two cases, manual segmentation of vessel ROIs or manual selection of the pulmonary perfusion phase was necessary.

A significant contrast between normally and poorly perfused lung areas was seen on PREFUL perfusion images. The normalized perfusion, expressed as percentage, was found to be 5.6% (SD 3.8%) for normally perfused ROIs and 1.4% (SD 1.9%) for poorly perfused ROIs. The mean difference between normally and poorly perfused areas was 4.2% (SD 3.3%) and was statistically significant (see Fig. 3). Across study sites, no significant differences were observed in the estimated perfusion contrast (ANOVA: $F = 1.92$, $P = 0.065$).

QDP_{PREFUL} was significantly correlated with QDP_{DCE} ($r = 0.66$). The mean QDP_{PREFUL} was found to be 43.5% (SD 19.3%), while the mean QDP_{DCE} was found to be 45.2% (SD 12%). The difference in means between the two measures was 1.7% (SD 14.6%) and was not significant (paired *t*-test: $P = 0.447$, see Fig. 4).

QDP_{PREFUL} was significantly higher in patients with confirmed CTEPH/CTED when compared to other patients in the study cohort (mean QDP_{PREFUL} in the positive group = 57.9% SD 12.2% and mean QDP_{PREFUL} in the negative group = 33.9% SD 17.2%; Fig. 5). In patients with excluded CTEPH/CTED, a higher variance of QDP_{PREFUL} was found compared to patients with confirmed diagnosis of CTEPH/CTED (interquartile range [IQR] of QDP_{PREFUL} in patients with confirmed CTEPH/CTED = 43.8%–68.4% and in excluded CTEPH/CTED = 12.9%–59%).

VDP_{PREFUL} was not significantly different between patients with confirmed and excluded CTEPH/CTED (*t*-test: $P = 0.68$). However, VDP_{PREFUL} was significantly higher in patients with diagnosed COPD regardless of their PH status (see Fig. 5). In all patients, VDP_{PREFUL} correlated with three lung function testing parameters: FEV1 ($r = -0.37$), FEV1/FVC ($r = -0.361$), and TLC ($r = 0.548$). rFVL-CC correlated significantly only with TLC ($r = -0.392$). A total of four participants from two study centers could not be included in the latter analysis due to lacking lung function testing. One study center did not report TLC measurements, so their five participants could not be included in the comparison with TLC.

Discussion

The aim of this work was to assess the feasibility of using PREFUL-MRI in a standardized multicenter study. By analyzing a cohort of 45 patients with suspected CTEPH who participated in the European CHANGE-MRI study, differences were found in MR image quality between different study centers in terms of quantitative measures (SNR and CNR). However, the MR image quality was rated as diagnostic for all datasets. PREFUL perfusion maps from all study centers have shown a good contrast between normally and poorly perfused areas. PREFUL estimation of ventilation defects correlated significantly with lung function testing parameters.

Previous studies have already validated the use of PREFUL-MRI for assessing regional lung function.[2–4,19] This work provided additional evidence that PREFUL-MRI can quantify regional lung perfusion and ventilation in a multicenter setting, even when differences in quantitative parameters of raw image quality (SNR and CNR) are seen. The automated analysis pipeline of this study performed all PREFUL post-processing steps on datasets acquired in different study centers using different MRI scanners. Some coronal slices showed mild to moderate registration inaccuracies probably due to partial volume effect (all these slices were positioned in most anterior or posterior planes in the lung). Only a small portion of the datasets required manual correction of

15222586, 0, Downloaded from https://onlinelibrary.wiley.com/doi/10.1002/jmri.28995 by Test, Wiley Online Library on [27/09/2023]. See the Terms and Conditions (https://onlinelibrary.wiley.com/terms-and-conditions) on Wiley Online Library for rules of use; OA articles are governed by the applicable Creative Commons License

15222586, 0, Downloaded from https://onlinelibrary.wiley.com/doi/10.1002/jmri.28995 by Test, Wiley Online Library on [27/09/2023]. See the Terms and Conditions (https://onlinelibrary.wiley.com/terms-and-conditions) on Wiley Online Library for rules of use; OA articles are governed by the applicable Creative Commons License

FIGURE 2: Boxplots of SNR and CNR of raw PREFUL images in end inspiration and end expiration across all study sites. *P*-values represent the result from the center-wise paired t-test.

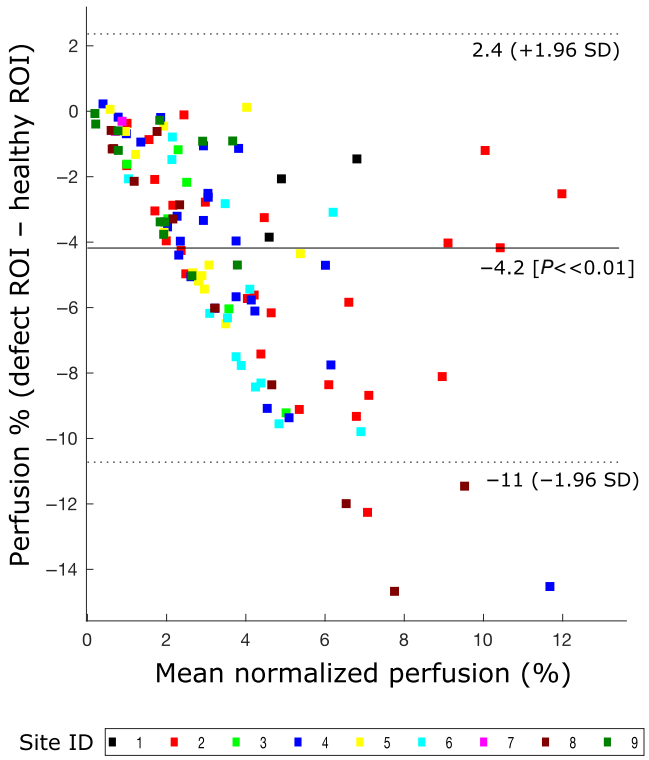

FIGURE 3: Bland–Altman plot of normalized lung perfusion on PREFUL images between areas with normal perfusion and others with perfusion defects that were segmented in accordance with the VQ-SPECT scans. Datapoints (each from a coronal slice in the dataset) are plotted with different colors according to the corresponding study center (see Table 1).

automated lung segmentation, while a larger proportion required manual vessel ROI segmentation and selection of lung perfusion phase. Further technical developments of the automated pipeline could benefit greatly from the availability of multicenter datasets. This would enable the development of a more reliable fully-automated post-processing pipeline that would facilitate the implementation of PREFUL-MRI in clinical routine.

Although a voxel-to-voxel comparison of PREFUL maps to perfusion scintigraphy could not be performed due to inconsistencies in the storage of VQ-SPECT images, the results of this study showed the feasibility of detecting lung areas of hypoperfusion using PREFUL-MRI in a multicenter setting. These findings were in accordance with the perfusion defects seen on SPECT imaging. First, there was a significant contrast between normally and poorly perfused areas on the PREFUL perfusion map with no significant differences between study centers. Second, estimated QDP values using PREFUL were significantly correlated to those calculated from the widely used DCE technique. The correlation coefficient was similar to that reported in a previous dual-center study in patients with cystic fibrosis.[4] In addition, patients with diagnosed CTEPH (or CTED) had, as expected, a significantly higher QDP_{PREFUL} than those with a negative CTEPH diagnosis. The CTEPH negative group included some participants with a relatively high QDP, who were clinically ill and could have pulmonary perfusion deficits due to other causes, such as severe emphysema. The group of

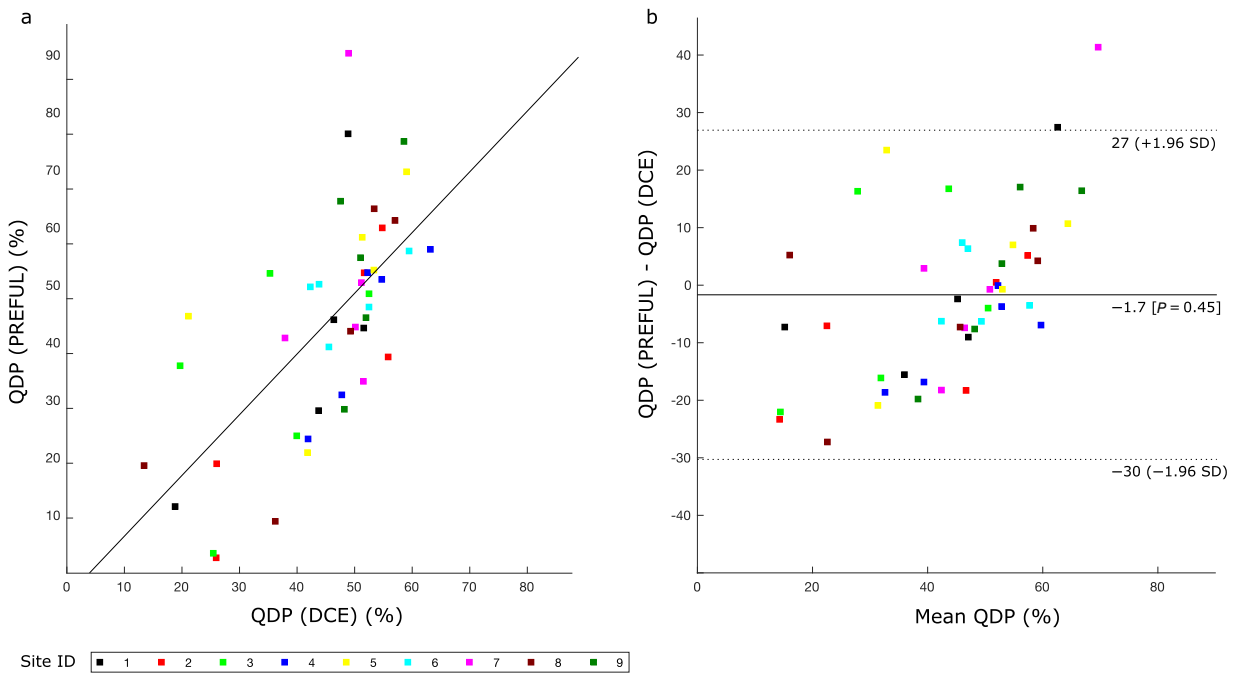

FIGURE 4: Depiction of the correlation between QDP_{PREFUL} and QDP_{DCE}. (a) Scatter plot with a regression line and (b) Bland–Altman plot showing the mean difference (solid line) and the ±1.96 SD (dotted lines). Datapoints (each from a coronal slice in the dataset) are color coded according to the corresponding study-center as specified in Table 1. QDP_{PREFUL}/QDP_{DCE}: perfusion defect percentage calculated using phase-resolved functional lung (PREFUL-MRI)/dynamic contrast-enhanced MRI (DCE-MRI).

15222586, 0, Downloaded from https://onlinelibrary.wiley.com/doi/10.1002/jmri.28995 by Test, Wiley Online Library on [27/09/2023]. See the Terms and Conditions (https://onlinelibrary.wiley.com/terms-and-conditions) on Wiley Online Library for rules of use; OA articles are governed by the applicable Creative Commons License

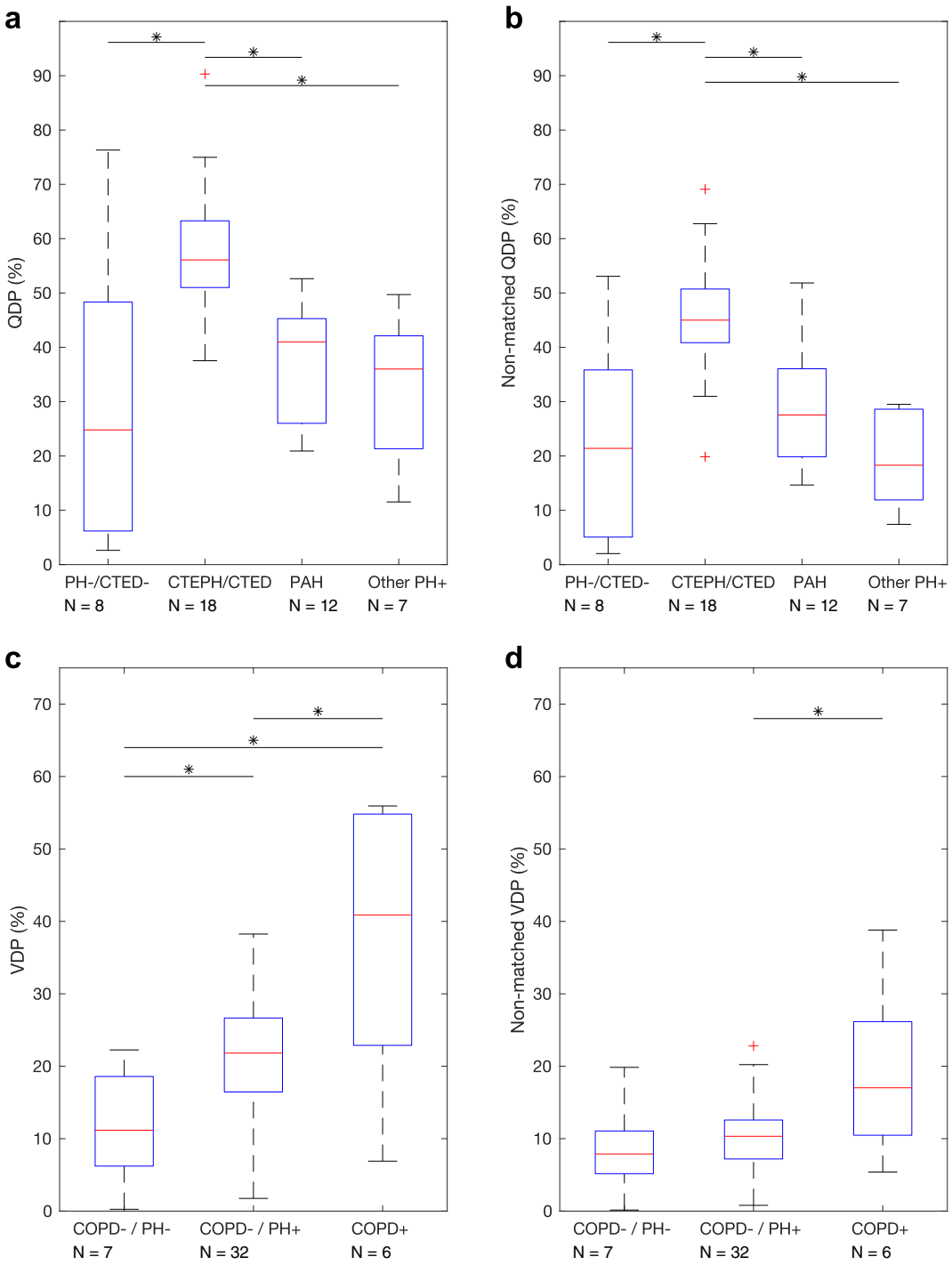

FIGURE 5: Boxplots of (a) QDP_{PREFUL}, (b) non-matched QDP_{PREFUL}, (c) VDP_{PREFUL}, and (d) non-matched VDP_{PREFUL} in different clinical subgroups of the study participants. For QDP, a patient subgroup with confirmed CTEPH/CTED diagnosis and thus expected perfusion deficits were compared to other subgroups: pulmonary arterial hypertension (PAH), other causes of pulmonary hypertension (Other PH+) and excluded pulmonary hypertension/excluded CTED (PH−/CTED−). VDP was compared between a patient subgroup with diagnosed COPD (expected ventilation defects) and subgroups with no COPD and either a confirmed or excluded PH (COPD−/PH+ or COPD−/PH−, respectively). Asterisks represent significant differences. Red lines indicate the median and whiskers indicate the variability outside the upper and lower quartiles.

patients with confirmed pulmonary arterial hypertension (PAH) rather than CTEPH showed also a high QDP. This could be a result of increased precapillary pulmonary arteriolar resistance in the PAH group, causing a delayed peak of the estimated pulse wave with decreased amplitude in the lung capillaries.

In all centers, a significant difference in lung SNR was found between inspiration and expiration, hence, an

15222586, 0, Downloaded from https://onlinelibrary.wiley.com/doi/10.1002/jmri.28995 by Test, Wiley Online Library on [27/09/2023]. See the Terms and Conditions (https://onlinelibrary.wiley.com/terms-and-conditions) on Wiley Online Library for rules of use; OA articles are governed by the applicable Creative Commons License

estimation of regional lung ventilation using PREFUL was expected to be technically possible.[1] A significant correlation of the estimated ventilation defect percentage with lung function further confirmed this hypothesis. As expected, no significant difference in VDP_{PREFUL} was found between positive and negative CTEPH groups. However, patients with an obstructive lung disease showed significantly higher VDP_{PREFUL} than others without known COPD, regardless of an accompanying PH or not.

The fact that the 1.5 T GE MRI scanner showed significantly lower SNR and CNR values in the lung parenchyma compared to the 1.5 T Siemens scanners despite even a lower matrix size used on GE may be explained by inherent vendor differences of the hardware and software despite using GRE FLASH sequences on all scanners. Nevertheless, also on the GE MRI significant differences between in- and expiration could be observed with resulting diagnostic PREFUL-derived ventilation and perfusion maps.

Limitations

One limitation of this work was the low number of subjects from each study center. Furthermore, no direct comparison of PREFUL parameters of the same patient scanned at different sites was possible because each participant was examined only once at a specific study center.

Conclusion

PREFUL-MRI could be considered as a standardized method for examining regional lung function in multicenter studies.

Acknowledgments

We thank Milan Speth for his contribution to the data assessment. This work was supported by a grant from the German Center for Lung Research (DZL).

References

1. Voskrebenzev A, Gutberlet M, Klimeš F, et al. Feasibility of quantitative regional ventilation and perfusion mapping with phase-resolved functional lung (PREFUL) MRI in healthy volunteers and COPD, CTEPH, and CF patients. Magn Reson Med 2018;79:2306-2314.
2. Behrendt L, Voskrebenzev A, Klimeš F, et al. Validation of automated perfusion-weighted phase-resolved functional lung (PREFUL)-MRI in patients with pulmonary diseases. J Magn Reson Imaging 2020;52: 103-114.
3. Pöhler GH, Klimes F, Voskrebenzev A, et al. Chronic thromboembolic pulmonary hypertension perioperative monitoring using phase-resolved functional lung (PREFUL)-MRI. J Magn Reson Imaging 2020;52: 610-619.
4. Behrendt L, Smith LJ, Voskrebenzev A, et al. A dual center and dual vendor comparison study of automated perfusion-weighted phase-resolved functional lung magnetic resonance imaging with dynamic contrast-enhanced magnetic resonance imaging in patients with cystic fibrosis. Pulm Circ 2022;12:e12054.
5. Moher Alsady T, Voskrebenzev A, Greer M, et al. MRI-derived regional flow-volume loop parameters detect early-stage chronic lung allograft dysfunction. J Magn Reson Imaging 2019;50:1873-1882.
6. Marshall PS, Kerr KM, Auger WR. Chronic thromboembolic pulmonary hypertension. Clin Chest Med 2013;34:779-797.
7. Simonneau G, Torbicki A, Dorfmüller P, Kim N. The pathophysiology of chronic thromboembolic pulmonary hypertension. Eur Respir Rev 2017; 26:160112.
8. Wilkens H, Konstantinides S, Lang IM, et al. Chronic thromboembolic pulmonary hypertension (CTEPH): Updated recommendations from the Cologne consensus conference 2018. Int J Cardiol 2018;272S:69-78.
9. Quadery SR, Swift AJ, Billings C, et al. P183 impact of patient choice on survival in patients with chronic thromboembolic pulmonary hypertension offered pulmonary endarterectomy. Pulmonary vascular disease: Monitoring and managing. 2017.
10. Kawakami T, Matsubara H, Shinke T, et al. Balloon pulmonary angioplasty versus riociguat in inoperable chronic thromboembolic pulmonary hypertension (MR BPA): An open-label, randomised controlled trial. Lancet Respir Med 2022;10:949-960.
11. Humbert M, Kovacs G, Hoeper MM, et al. 2022 ESC/ERS guidelines for the diagnosis and treatment of pulmonary hypertension. Eur Respir J 2023;61:3618-3731.
12. Helmersen D, Provencher S, Hirsch AM, et al. Diagnosis of chronic thromboembolic pulmonary hypertension: A Canadian Thoracic Society clinical practice guideline update. Can J Respir Crit Care Sleep Med 2019;3:177-198.
13. Johns CS, Swift AJ, Rajaram S, et al. Lung perfusion: MRI vs. SPECT for screening in suspected chronic thromboembolic pulmonary hypertension. J Magn Reson Imaging 2017;46:1693-1697.
14. Rajaram S, Swift AJ, Telfer A, et al. 3D contrast-enhanced lung perfusion MRI is an effective screening tool for chronic thromboembolic pulmonary hypertension: Results from the ASPIRE Registry. Thorax 2013; 68:677-678.
15. Lasch F, Karch A, Koch A, et al. Comparison of MRI and VQ-SPECT as a screening test for patients with suspected CTEPH: CHANGE-MRI study design and rationale. Front Cardiovasc Med 2020;7:51.
16. Voskrebenzev A, Gutberlet M, Kaireit TF, Wacker F, Vogel-Claussen J. Low-pass imaging of dynamic acquisitions (LIDA) with a group-oriented registration (GOREG) for proton MR imaging of lung ventilation. Magn Reson Med 2017;78:1496-1505.
17. Avants BB, Tustison NJ, Song G, Cook PA, Klein A, Gee JC. A reproducible evaluation of ANTs similarity metric performance in brain image registration. Neuroimage 2011;54:2033-2044.
18. Ronneberger O, Fischer P, Brox T: U-Net: Convolutional networks for biomedical image segmentation. Lecture Notes in Computer Science. 2015. p 234–241.
19. Kaireit TF, Voskrebenzev A, Gutberlet M, et al. Comparison of quantitative regional perfusion-weighted phase resolved functional lung (PREFUL) MRI with dynamic gadolinium-enhanced regional pulmonary perfusion MRI in COPD patients. J Magn Reson Imaging 2019;49: 1122-1132.
20. Constantinides CD, Atalar E, McVeigh ER. Signal-to-noise measurements in magnitude images from NMR phased arrays. Magn Reson Med 1997;38:852-857.

15222586, 0, Downloaded from https://onlinelibrary.wiley.com/doi/10.1002/jmri.28995 by Test, Wiley Online Library on [27/09/2023]. See the Terms and Conditions (https://onlinelibrary.wiley.com/terms-and-conditions) on Wiley Online Library for rules of use; OA articles are governed by the applicable Creative Commons License